Eur. Phys. J. A **17**, 339–343 (2003)
DOI 10.1140/epja/i2002-10201-y

THE EUROPEAN PHYSICAL JOURNAL A

Parity-violating electron scattering at the MAMI facility in Mainz

The strangeness contribution to the form factors of the nucleon

F.E. Maas[a]

For the A4 Collaboration
Johannes Gutenberg Universität Mainz, Institut für Kernphysik, J.J. Becherweg 45, 55299 Mainz, Germany

Received: 1 November 2002 /
Published online: 15 July 2003 –

Abstract. We report here on a new measurement of the parity-violating (PV) asymmetry in the scattering of polarized electrons on unpolarized protons performed at the MAMI accelerator facility in Mainz. This experiment is the first to use counting techniques in a parity violation experiment. The kinematics of the experiment is complementary to the earlier measurements of the SAMPLE Collaboration at the MIT-Bates accelerator and the HAPPEX Collaboration at Jefferson Lab. After discussing the experimental context of the experiments, the setup at MAMI and preliminary results are presented.

PACS. 12.15.-y Electroweak interactions – 25.30.Bf Elastic electron scattering

1 Strangeness

1.1 Strangeness in the nucleon

The structure of the nucleon is often described in terms of three constituent quarks where these are understood as effective particles with a mass that arises dynamically from a sea of virtual gluons and virtual quark-antiquark pairs. The contribution of the strange quarks to this sea is of special interest, since the mass value of the strange quarks is approximately equal to the scale of λ_{QCD} and lies in between the masses of the very light u and d current quarks and the mass of the much heavier quarks like c, b and t. There is a detailed discussion of the present understanding of the role of strangeness within the nucleon in the literature [1,2].

Unfortunately, the scalar strangeness density $\overline{s}s$ does not couple directly to the electromagnetic probe; therefore the answer on the question of how much strangeness is in the nucleon is not directly available. The analysis of the scattering amplitude in πN-scattering and the connection to the Σ_π term and the scalar density matrix element $\langle N|\,\overline{s}\,s\,|N\rangle$ gives a contribution of the strange quark-antiquark pairs to the mass of the nucleon on the order of 130 MeV [3]. New data from πN-scattering suggest even a larger value up to 50% of the proton mass. The observed charm production rate from deep inelastic neutrino nucleon scattering can only be explained if there is a 2% contribution of the strange quarks to the momentum of the nucleon. In polarized deep inelastic muon and electron scattering the axial matrix element $\langle N|\,\overline{s}\,\gamma^\mu\gamma^5 s\,|N\rangle$ is measured. It is equal to the contribution of the strange quarks to the spin of the proton Σ_s. A value for Σ_s of 0.12 ± 0.1 has been extracted [4]. Our experiment aims at a measurement of the contribution of strange quark-antiquark pairs to the elastic vector form factors of the nucleon.

[a] e-mail: maas@kph.uni-mainz.de

1.2 Extracting the strangeness form factor contribution

The dynamic response of the nucleon structure to electron scattering via the exchange of virtual photons is described in terms of the four elastic form factors: the Dirac form factor $F_1^{p,n}(Q^2)$ of proton and neutron and the Pauli form factor $F_2^{p,n}(Q^2)$ (another combination are the Sachs form factors, $G_E^{p,n} = F_1^{p,n} - \tau F_2^{p,n}$ and $G_M^{p,n} = F_1^{p,n} + F_2^{p,n}$). It has been first noted by Caplan and Manohar [5], that a flavor decomposition of the form factors into the three lightest quark flavors u, d and s can be obtained. This is obtained by combining the form factors of proton and neutron using isospin symmetry and electromagnetic and weak neutral current form factors. If one writes the electromagnetic ($F_{1,2}^{p,n}$) and the weak form factors ($\tilde{F}_{1,2}^{p,n}$) decomposed into the three lightest quark flavors, one obtains

$$F_{1,2}^{p,n} = Q_u\,{}^u F_{1,2}^{p,n} + Q_d\,{}^d F_{1,2}^{p,n} + Q_s\,{}^s F_{1,2}^{p,n}\,, \tag{1}$$

$$\tilde{F}_{1,2}^{p,n} = \tilde{Q}_u\,{}^u \tilde{F}_{1,2}^{p,n} + \tilde{Q}_d\,{}^d \tilde{F}_{1,2}^{p,n} + \tilde{Q}_s\,{}^s F_{1,2}^{p,n}\,. \tag{2}$$

The left side of eqs. (1) and (2) represents the eight experimentally accessible electromagnetic and weak form factors of the nucleon and on the right side are the 12 unknown

flavor contributions. The Q-factors are the electromagnetic and weak charges of the appropriate quark flavor, *i.e.* the electric and the weak charge of quark flavors u, d and s. Isospin symmetry allows to eliminate one half of the unknown quark flavor contributions by replacing the u-quark contributions in the proton by the d-quark contribution in the neutron (${}^uF^p_{1,2} = {}^dF^n_{1,2} \rightarrow {}^uF_{1,2}$, ${}^sF^p_{1,2} = {}^sF^n_{1,2} \rightarrow {}^sF_{1,2}$) and vice versa and to use one strangeness contribution for both proton and neutron. In addition, the quark distributions are an intrinsic property of the nucleon and do not depend on the probe. This allows to use the same flavor form factor contributions in eqs. (1) and (2) (${}^{u,d,s}F_{1,2} = {}^{u,d,s}\tilde{F}_{1,2}$). Therefore, the number of unknown flavor contributions on the right side of eqs. (1) and (2) is now reduced down to 6 unknown flavor contributions ${}^{u,d,s}F_{1,2}$, which can be determined, provided the electromagnetic and weak neutral form factors are measured by experiment.

The weak neutral form factors enter into the amplitude M for elastic scattering of electrons off protons

$$A^{\mathrm{PV}} = \frac{\sigma_R - \sigma_L}{\sigma_R + \sigma_L} \tag{3}$$

$$= \left[\frac{-G_F Q^2}{2\pi\alpha\sqrt{2}}\right] \times \frac{\epsilon G_E^p \tilde{G}^p{}_E + \tau G_M^p \tilde{G}_M^p - \frac{1}{2}(1-4\sin^2\theta_W)\epsilon' G_M^p \tilde{G}_A}{\epsilon {G_E^p}^2 + \tau {G_M^p}^2} \tag{4}$$

$$= \left[\frac{-G_F Q^2}{2\pi\alpha\sqrt{2}}\right] \times \left\{ (1-4\sin^2\theta_W) + \frac{\epsilon G_E^p G_E^n + \tau G_M^p G_M^n}{\epsilon {G_E^p}^2 + \tau {G_M^p}^2} \right. \tag{5}$$

$$+ \frac{\epsilon G_E^p G_E^s + \tau G_M^p G_M^s}{\epsilon {G_E^p}^2 + \tau {G_M^p}^2} \tag{6}$$

$$\left. - \frac{\frac{1}{2}(1-4\sin^2\theta_W)\epsilon' G_M^p \tilde{G}_A}{\epsilon {G_E^p}^2 + \tau {G_M^p}^2} \right\}, \tag{7}$$

which is described at lowest order (one-boson exchange) by the sum M of the pure–γ-exchange amplitude m_γ and the pure neutral current Z_0-exchange amplitude m_{Z_0}. The cross-section is given by the square of the amplitude $M\,M^*$ and consists of three terms: the pure γ-exchange ($m_\gamma m^*_\gamma$), the γ-Z_0 interference term ($m_\gamma m^*_{Z_0}$) and the pure Z_0-exchange ($m_{Z_0} m^*_{Z_0}$). At the proton vertex the elastic electromagnetic and weak form factors enter and can therefore be measured in electron scattering. In elastic electron proton scattering at four-momentum transfer in the range $0.1\ \mathrm{GeV}^2 < Q^2 < 1\ \mathrm{GeV}^2$ the γ-Z_0 interference term is about 5 orders of magnitude smaller than the pure γ-exchange. The direct measurement of the weak contribution to the cross-section is therefore at present beyond experimental reach. But the parity-violating coupling of the Z_0 gives a unique possibility to separate the pure γ-exchange from the interference term. In a measurement of the parity-violating asymmetry in elastic scattering of longitudinally polarized electrons on unpolarized protons the pure γ-exchange ($m_\gamma m^*_\gamma$) vanishes and one measures directly the interference term. Therefore, one has direct access to the weak form factors of the nucleon, since the electromagnetic form factors are known from other experiments. As we have seen above, the determination of the weak form factors is equivalent to the determination of the strangeness contribution to the vector form factors of the nucleon. The experimental quantity which is measured is the difference in the cross-section in the scattering of left-handed or right-handed electrons on unpolarized protons divided by the sum of the two cross-sections. This is a parity-violating asymmetry which can be calculated in the framework of the standard model. Here $\tau = \frac{Q^2}{4M_p^2}$ and $\epsilon = (1 + 2(1+\tau)\tan^2(\frac{\theta}{2}))^{-1}$ and $\epsilon' = \sqrt{\tau(1+\tau)(1-\epsilon^2)}$. Using the flavor decomposition of eq. (1), the asymmetry in eq. (5) can be written like eq. (5) as the sum of three terms (5), (6) and (7). (5) contains fundamental constants and the electromagnetic form factors only. (5) is often referred to as A_0. (6) contains the unknown strangeness contribution to the vector form factors of the nucleon. (7) contains the weak axial form factor G_A which is known only at $Q^2 = 0\ \mathrm{GeV}^2$ from neutron beta-decay. In forward scattering (7) is strongly suppressed due to the kinematical factors. The sensitivity on the axial term is on the order of 1-2% for HAPPEX and A4 kinematics. In the case of backward scattering the sensitivity to the axial form factor is of the same order as the sensitivity to the magnetic form factor, the determination of term (7) requires an additional measurement of the parity-violating asymmetry A^{PV} on deuterium. Any significant difference between the measured parity-violating asymmetry A and A_0 is in forward scattering a direct measure of the strangeness contribution to the vector form factors of the nucleon.

Table 1. The different experimental approaches to separate inelastic- from elastic-scattering processes at the very high scattered particle flux have been optimized to meet the specific kinematical requirements of each of the experiments.

Experiment	Elastic ↔ Inelastic	Measurement of high rate
SAMPLE [6–9]	Low energy, no π-production	Integrating, air Čerenkov
HAPPEX [10–14]	Magnetic spectrometer	Integrating, in focal plane
A4 [15]	Crystal calorimeter (E)	Counting, histogramming E
G0 [16]	Time of flight (T)	Counting, histogramming T

2 Experimental approaches

In parity violation electron scattering one finds two experimental difficulties and the existing experiments use different techniques to overcome these as summarized in table 1. First difficulty is the size of the asymmetry without strangeness contribution A_0 in eq. (5) which is used

as an estimate of the expected measured asymmetry. For the existing and planned experiments it is on the order of $A_0 \approx 10^{-6}$. A significant determination of the strangeness contribution requires a measurement at a very high rate of elastic scattered electrons in order to determine the asymmetry in reasonable experimental time with an accuracy of a few percent. Second, in the applied Q^2 range of the existing and planned experiments, one has inelastic channels like nonresonant π-electroproduction or excitations of nucleon resonances like the Δ. These inelastic channels have to be separated very well from the elastic scattering, since they have their own parity-violating asymmetries which are *a priori* unknown.

The SAMPLE Collaboration has measured [6–8] at the MIT-Bates accelerator under backward-scattering angles between 130° and 170° using a large solid-angle air Čerenkov detector. The status of the experimental results from the previous proton and deuterium measurements is described in this volume.

The Hall A Proton Parity EXperiment (HAPPEX) Collaboration has measured parity violation in electron scattering at Jefferson Laboratory using the two spectrometers in Hall A. Both identical spectrometers have been used symmetrically and have been set to very forward-scattering angles ($\theta = 12.3°$). The scattered elastic electrons have been selected using a lucite-lead detector sitting in the focal plane of the spectrometer. The shape of the calorimeter has been adjusted to detect elastic scattered electrons only, which are in the focal plane very well separated from the inelastic channels. The measured asymmetry is [10,11]

$$A_p(Q^2 = 0.477\ \mathrm{GeV}^2) = (-14.60 \pm 0.94 \pm 0.54)\,\mathrm{ppm}\,. \quad (8)$$

The experiment is sensitive to the form factor combination $G_E^s + 0.392 G_M^s$. The contribution from the axial form factor had been estimated from calculation [17] to (-0.56 ± 0.23) ppm. The value of the strangeness contribution to the asymmetry has been normalized to the proton magnetic form factor and is

$$\frac{G_E^s + 0.392 G_M^s}{G_M^p/\mu^p} = 0.091 \pm 0.054 \pm 0.039\,. \quad (9)$$

The HAPPEX Collaboration is planning two further measurements: A measurement at a lower Q^2 of 0.1 GeV^2 [12] which then gives a different combination of G_E^s and G_M^s. The second proposal [13] is a measurement with elastic scattering from ^{4}He where all magnetic and axial contributions cancel giving a very clean measurement of G_E^s. The G0 Collaboration [16] at Hall C of TJNAF is a new experiment, which is currently set up and will start data taking in 2003. The experiment uses a large solid-angle toroidal magnetic spectrometer. It detects the elastic scattered protons and uses their time of flight in order to discriminate them from inelastic background processes.

2.1 The A4 Collaboration at the MAMI facility in Mainz

The A4 Collaboration [15] has performed a measurement of the parity-violating asymmetry in the scattering of longitudinally polarized 854.3 MeV electrons on unpolarized protons using counting techniques. This is the first time that a parity-violating asymmetry in electron scattering has been measured by counting individual, scattered particles. Particles scattered from the hydrogen target are detected between $30° < \theta < 40°$ (0.7 srad), resulting in a Q^2 at 35° of 0.23 GeV^2. The particle rate of elastic scattered electrons in the solid angle of the detector is about 10 MHz, where the energy of the elastically scattered electrons is 734 MeV at 35° scattering angle. In addition there is an almost ten times higher background of about 90 MHz coming from other processes. Scattered electrons from pion production are closest in energy to elastic scattered electrons (610 MeV at 35°). Since the pion production has an unknown parity-violating asymmetry by itself, the energy resolution of the PbF_2-detector has to be good enough to separate these two processes at a level better than 1%. Some of the photons from π^0-decay can carry almost the energy of an elastic electron due to the three-body π-production and additional boost [18]. The principle of the experimental setup can be divided in three different parts: 1) The electron source with the subsequent MAMI accelerator is the first and important part of the experiment. Helicity-correlated changes of beam parameters cause trivial asymmetries in the PbF_2-detector and therefore need to be suppressed with substantial effort already at the electron source and within the electron accelerator. 2) The fast fully absorbing PbF_2-Čerenkov calorimeter with the high-power hydrogen target and the luminosity monitor detect the flux of particles and measure the particle energy. 3) In the associated experiment readout electronics the particles are registered and histogrammed with a dead time of 20 ns according to their deposited energy in order to separate elastic scattered electrons from other inelastic channels like π-production.

Electrons from a high polarization strained layer GaAs crystal at a current of 20 μA and with a longitudinal polarization of about 80% are accelerated within the three stages of the MAMI racetrack microtron up to an energy of 854.3 MeV. A fast reversal at about 25 Hz of the electron polarization is achieved by a Pockels cell, which reverses the circular polarization of the laser light hitting the GaAs crystal. An additional slow reversal of the electron polarization is done by putting in or out an additional $\lambda/2$-plate in the optical system (GVZ). The electron current at the source is stabilized in a closed feedback loop by measuring the electron current in front of the high-power hydrogen target and modulating the power of the laser light hitting the GaAs crystal. Independently, any difference in the electron current for the two different helicity states is controlled to a level of several ppm by adjusting the angle of an additional permanently installed $\lambda/2$-plate. The energy of the electron beam is stabilized and controlled to a level of $\Delta E/E = 10^{-6}$ by measuring the phase advance of the electrons in the last turn of the third stage of

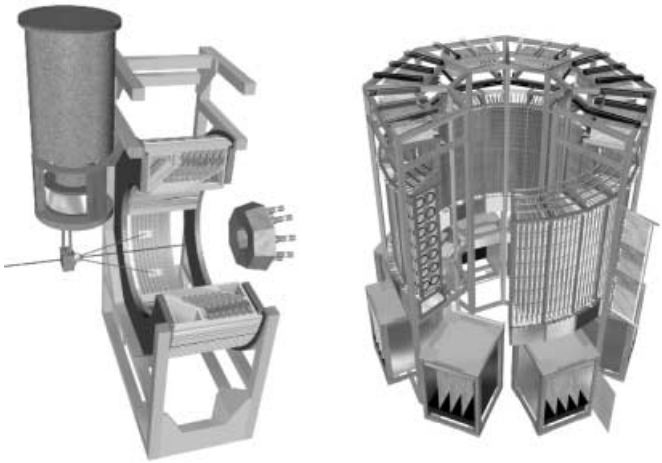

Fig. 1. The left side shows a schematic of the mechanical setup of the lead fluoride calorimeter. The electron beam coming from the left is at about 2.2 m height. The right side is a schematic of the mechanical setup of the associated readout electronics which is in total about 3 m high.

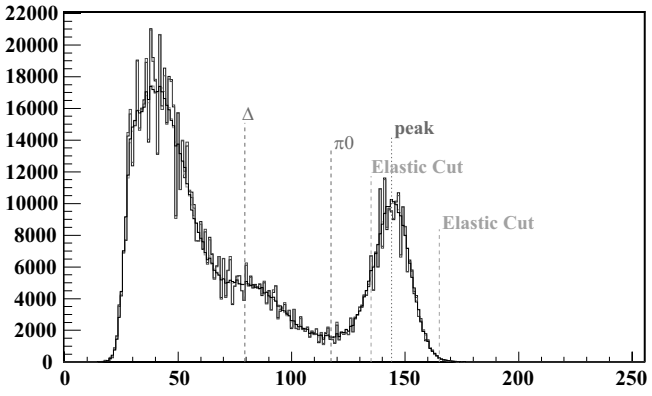

Fig. 2. The data show an energy spectrum of scattered particles from the hydrogen target as read directly from the hardware memory. The number of counts per channel is displayed *versus* the ADC channel. The only correction comes from the differential nonlinearity of the ADC.

MAMI by heterodyne methods and modulating the phase of the accelerating microwaves in the third-stage linacs. In order to stabilize and control the position and the angle of the electron beam, the horizontal and vertical position of the electron beam is measured at two locations separated by 10 m in front of the hydrogen target by using position-sensitive microwave cavities. The position signal is feedback to fast modulating coils, which then stabilize position and angle of the beam. The stabilization systems within the accelerator and the beam line have made it possible to efficiently suppress false asymmetries in the PbF_2-detector. The mean of the helicity-correlated variation of individual beam parameters over a data sample corresponds to false asymmetries in the PbF_2-detector which are less than 0.05 ppm or less than 1% of the expected asymmetry in the PbF_2-detector.

The target system is a special new design, which enforces turbulent flow in the target cell, so that the effective heat conductance is enhanced by transverse flow. The target can stand without boiling the full 20 μA of electron beam current also without any rastering of the electron beam. The left part of fig. 1 shows a design drawing of the 1022 channel PbF_2-Čerenkov calorimeter. For the measurements presented here, only half of the 1022 detector and electronics channels had been installed. The completion of the solid angle is in progress and almost completed. Scattered electrons coming from the left (electron beam height: 2.2 m) pass through the high-power liquid-hydrogen target. The scattered particles produce an electromagnetic shower in a cluster of lead fluoride crystals. The crystals have a length of 16–20 radiation lengths and a width of about $\frac{4}{3}$ of a Moliere radius so that the full electromagnetic shower of an elastic scattered electron is contained in a 3×3 crystal cluster. The Čerenkov light is read out by photomultiplier tubes. Eight water-Čerenkov luminosity monitors are located ϕ-symmetrically under a scattering angle of 4–10°, where the asymmetry from elastic scattering is negligible.

The right part of fig. 1 shows the mechanical setup of the associated 3 m high readout electronics, which consists of 1022 identical readout channels and which has been developed in the Institut für Kernphysik in Mainz. The photomultiplier signals of every 3×3 cluster are summed in a summation amplifier, integrated over 20 ns, digitized with a fast digitizer and stored in a fast first-in–first-out pipeline chip. A local maximum signal is derived by comparing the signal of the center crystal with the 4 direct neighbors. The additional requirement of an energy deposit above a threshold triggers the fast digitization. Any second particle hitting the same cluster or any direct neighboring cluster within the integration time of 20 ns would hinder the determination of the energy of the scattered particle and is therefore vetoed by the veto circuit. In this circuit the local maximum signals from the 5×5 cluster around the central 3×3 cluster need to be controlled. The distribution of the analogue and digital signals is done by a special bus structure where every detector module is connected to the 8 neighboring modules for the analogue signals and where every veto circuit is connected to the 24 neighboring modules for the digital signals. This requires also that the topology of the electronics is the same as the detector, *i.e.* neighboring detector modules go into neighboring electronics channels. The registered events in the pipeline are histogrammed in hardware memory in VME-bus–based modules. The upper part of fig. 1 right contains the analogue sum, the trigger and veto circuit and the digitization, the lower part contains the galvanically separated VME-bus–based histogramming circuits. The whole lead fluoride detector is a completely new development and is used here for the first time. The whole system of electronics and detector achieves an energy resolution of 3.5% at 1 GeV and a total dead time of 20 ns. The average rate per channel is about 500 kHz.

Figure 2 shows a histogram of the scattered particle energies as read out from the histogramming memory of the data acquisition electronics. One can see the peak of elastic scattered electrons in the right part of the spectrum. There is a distinct valley between the elastic scattering and the

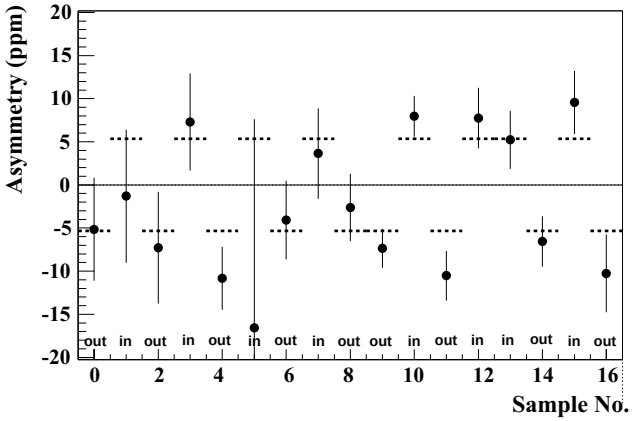

Fig. 3. The measured decorrelated polarization corrected asymmetries are shown with the $\lambda/2$-plate in or out, respectively, as a function of the data sample.

Δ-excitation. At lower energies Moeller and Moeller-Mott scattering and excitation of higher resonances are the main sources of the background. The leftmost part of the spectrum is defined by the discriminator threshold. There are at present 1022 histograms (511 for each polarization direction) per 5 minutes run which give at present a total of about 10 000 000 histograms. These histograms together with the recorded beam parameters represent the data set for the analysis. The number of scattered elastic electrons is determined by integrating the histogram between the lower and the upper elastic cut. The number of elastic scattered events is then normalized to the luminosity signal. In a final step, the correlation of the cross-section with the change of electron beam parameters is analyzed by a standard multidimensional regression analysis in order to determine the measured asymmetry in elastic scattering. The polarization of the electron beam has been measured with a Moeller polarimeter in the hall of the 3-spectrometer setup, where the electron beam is antiparallel with respect to the A4 beam line. The Moeller polarimeter itself has a high accuracy of about 2% per measurement. The fact that one has to interpolate between two measurements leads to a reduction in the knowledge of the polarization, which is reflected in an enlarged error on the polarization. Figure 3 shows the final decorrelated, polarization corrected asymmetry as a function of the data sample. The data samples have been taken in a period from November 2000 until June 2001 and April 2002. The dependence of the combined decorrelated asymmetry value on different parameters which are used to select PbF_2-spectra or to reject runs because of instable beam conditions etc. has been checked. It has been found that there is no significant variation of the asymmetry value on the different cut parameters. The combined preliminary result on the asymmetry from all data sets is

$$A_{\mathrm{exp}} = (-7.3 \pm 0.5 \pm 0.8) \times 10^{-6} \,. \qquad (10)$$

The first error is the pure statistical error coming form the counting statistics of the scattered particles. The second error is the combined systematical uncertainty from the regression analysis and the uncertainty in the polarizations.

The isolation of the individual electric or magnetic contribution is not possible with one measurement at this Q^2 value only. The further program of the A4 Collaboration involves the installation and commissioning of a laser backscatter Compton polarimeter and a transmission Compton polarimeter, which will reduce the uncertainty in the polarization from 7% down to possibly 2-3%. The completion of the missing 511 detector and electronics channels is also in progress and very important for the further measurement program. Due to the fact that we use crystals in the calorimeter, the Q^2 can be changed by changing the beam energy or by reverting the whole detector. This will make it possible to measure at a Q^2 of 0.1 GeV^2 in forward scattering ($\theta = (35 \pm 5)^\circ$) by lowering the beam energy to 570 MeV. In addition, the statistical and systematical error at the Q^2 value of 0.23 GeV^2 will be further reduced. The present planning foresees, that the whole detector will be reverted, so that the scattering angle will be changed to backward scattering between 140° and 150°. We plan measurements at $Q^2 = 0.23$ GeV^2 and $Q^2 = 0.47$ GeV^2 at this backward angle. In combination with the SAMPLE and HAPPEX measurements it will then be possible to make a full flavor separation at the three Q^2 values in order to reveal the contribution of the strangeness to the vector form factors of the proton.

This work has been supported by the Deutsche Forschungsgemeinschaft in the framework of the SFB 201, SPP 1034. We are indebted to K.H. Kaiser and the whole MAMI crew for their tireless effort to provide us with good electron beam. We are also indebted to the A1 Collaboration for the use of the Moeller polarimeter.

References

1. M.J. Musolf *et al.*, Phys. Rep. **239**, 1 (1994).
2. D.H. Beck, B. McKeown, Phys. Rev. D **36**, 2109 (1987).
3. B. Borasoy, U.-G. Meissner, Ann. Phys. **254**, 192 (1997).
4. H. Lipkin, M. Karliner, Phys. Lett. B **461**, 280 (1999).
5. D. Kaplan, A. Manohar, Nucl. Phys. B **310**, 527 (1988).
6. B.A. Mueller *et al.*, Phys. Rev. Lett. **78**, 3824 (1997).
7. D.T. Spayde *et al.*, Phys. Rev. Lett. **84**, 1106 (2000).
8. R. Hasty *et al.*, Science **290**, 2117 (2000).
9. T. Ito, MIT-Bates Lab experiments 00-04 (2000).
10. HAPPEX Collaboration (K.A. Aniol *et al.*), Phys. Rev. Lett. **82**, 1096 (1999).
11. HAPPEX Collaboration (K.A. Aniol *et al.*), Phys. Lett. B **509**, 211 (2001).
12. K. Kumar, D. Lhuillier, Jefferson-Lab experiment 99-115.
13. D. Armstrong, Jefferson-Lab experiment 00-114 (1999).
14. E. Beise, Jefferson-Lab experiment 91-004 (1991).
15. D. von Harrach, spokesperson, F.E. Maas contact. MAMI experiment A4-01-93.
16. D. Beck, Jefferson-Lab experiment 00-006 (2000).
17. S.L. Zhu *et al.*, Phys. Rev. D **62**, 033008 (2000).
18. S. Ong, M.P. Rekalo, J. Van de Wiele, Eur. Phys. J. A **6**, 215 (1999).